Spectroscopic Evidence for Interaction of Poly[2-methoxy-5-(2′-ethylhexyloxy)-1,4-phenylenevinylene] Conformers and Single-Walled Carbon Nanotubes in Solvent Dispersions

Christopher J. Collison,* Steven Pellizzeri, and Filip Ambrosio

Department of Chemistry, Rochester Institute of Technology, College of Science, 84 Lomb Memorial Drive, Rochester, New York 14623-5603

Received: December 19, 2008; Revised Manuscript Received: February 28, 2009

Organic photovoltaic devices promise low-cost, flexible options for future renewable energy that will reduce reliance on oil. Single-wall carbon nanotubes (SWCNTs) provide possibilities for increasing the efficiency of organic solar cells through increasing conductivity of composites used in such devices or through use as a charge acceptor in a bulk heterojunction device. We present data to indicate the physical interaction of SWCNTs with a conjugated polymer, poly[2′-methoxy-5-(2′-ethylhexyloxy)-1,4-phenylenevinylene] (MEH-PPV), on the basis of the spectroscopic assignments of various conformational species of different optical signature in *N*,*N*-dimethylacetamide (DMA) dispersions. We go on to show that energy transfer from nonaggregated MEH-PPV leads to enhanced SWCNT fluorescence in solutions of poorer solvent quality. Energy transfer from polymer chain lengths that are torsionally restricted is not observed. This would suggest that any electron transfer taking place is occurring through a concerted Dexter mechanism and that use of SWCNTs as an electron acceptor will likely have associated drawbacks.

Introduction

Organic photovoltaic devices promise low-cost, flexible options for future renewable energy that will reduce reliance on oil. Single-wall carbon nanotubes (SWCNTs) provide possibilities for increasing the efficiency of organic solar cells through increasing conductivity of composites used in such devices or through use as a charge acceptor in a bulk heterojunction device. The increase in device efficiency must be made while maintaining low-cost manufacturing advantages, leading to their widespread acceptance. The broader goal we choose to address in this paper is to improve the fundamental understanding of interactions between conducting polymers and SWCNTs, two important components of organic photovoltaic devices.

A substantial volume of work involving photovoltaic devices made of poly[2-methoxy-5-(2′-ethyl-hexyloxy)-1,4-phenylene vinylene] (MEH-PPV) and functionalized C_{60} fullerenes exists.[1] However, very little work has been done with energy transfer from MEH-PPV to carbon nanotubes, which offer distinct advantages through their extremely high aspect ratios and high electron mobility.[2,3]

In general, work involving carbon nanotubes in photovoltaic devices[4−6] appears minimal, perhaps because of shunting by exposed SWCNTs in direct contact with both electrodes. SWCNTs are somewhat difficult to make, separate, characterize, and process. SWCNTs are unreactive and suffer from low dispersion limits ("solubilities") in solvents. Studies have been conducted to measure ultimate device efficiencies.[7,2,8,9] Work also continues to better understand the interaction of SWCNTs with small molecules and solvents such that solvent processing of SWCNTs might be improved.[10] However, a strong understanding of the polymer−SWCNT interfaces is lacking.

In this work we consider the energy transfer of photoexcitation energy to the nanotube primarily from solvated single polymer chains. This "single molecule" solution approach will ultimately allow subsequent extrapolations to photovoltaic device efficiency to be made. Hence we benchmark the ability of the nanotubes to act as an acceptor in a photovoltaic device. We can exploit certain advantages by working in solution. The conformation of the conjugated polymer can be determined.[11] Furthermore, uncontrollable and complex spin-casting processes are eliminated. Ultimately, we hope to promote devices that are made by sparsely distributing SWCNTs inside polymer hosts, and it is important that we try to understand the interactions between single nanotubes or groups of nanotubes that are significantly debundled.

MEH-PPV is a straight-chain conjugated polymer. One might expect MEH-PPV to bind to SWCNTs, based on the chemical similarity of the conjugated backbones of both materials, and given the right solvent environment.[6] Ground state interactions between a fluorophore and a second material can be investigated if that second molecule acts as a fluorescence quencher. Quenching may occur through collisional interactions between quencher and fluorophore, where quencher must diffuse to fluorophore, or through the formation of a nonfluorescent complex. Despite there being evidence for both mechanisms we infer the formation of complexes between polymer and SWCNTs as providing a substantial degree of quenching.

Nish et al.[12] have provided evidence for energy transfer from MEH-PPV to nanotubes made in the "HiPCO" process.[13] The authors provide strong evidence for direct exciton transfer based on enhanced photoluminescence from nanotubes that are solubilized by different polymers. In fact, a model is proposed by Hwang et al.[14] (from the same group), for how different polymers wrap the SWCNT. Hwang claims that the more limits on the conformations that a polymer can adopt, the greater the selectivity for which nanotubes can be solubilized by that polymer. We wish to underline their conclusions but, in addition,

* To whom correspondence should be addressed. E-mail: cjcscha@rit.edu.

10.1021/jp811241v CCC: $40.75
Published on Web 04/03/2009

to measure which conformations (in the case of MEH-PPV) are more suitable for effective energy transfer.

Given the straight chain nature of MEH-PPV we might expect it to intrinsically remain stiff in solution on account of its phenylene-vinylene backbone, made up entirely of sp^2 hybridized carbons. However, in a range of solvents a broad change in the degree of packing can be observed along with an associated distribution of photophysical properties.[10] Traiphol et al.[15] have described at length the conformational states and their optical signatures that may be observed. We summarize them again here.

Aggregated MEH-PPV chains are registered along the backbone. These are described by Collison et al.[11] as "well-packed-registered" (WPR) chains. The characteristic photophysics of these multichain units are a red-shifted shoulder in the absorbance and red-shifted, long-lived fluorescence found at around 590 nm. Aggregates can be formed by reducing solvent quality or by increasing concentration.

Agglomerated chains are collections of chains where there is still an interchain association but the chains do not interact electronically.

Isolated chains (as observed in chloroform) demonstrate an emission peaking at 558 nm with a shoulder near 590 nm. When added to poor solvents some of these isolated MEH-PPV chains collapse around tetrahedral defects.[16−19] Presumably, these are the same tetrahedral defects that allow formation of conjugated polymer nanoparticles as described by Szymanski et al.[20] A broader absorption spectrum is observed as a result of the average conjugation length being smaller in collapsed chains; the broadening is manifested by a pronounced increase in absorption to the blue of the intrinsic 490 nm peak. However, energy transfer to the longer segments still occurs before emission and so the emission spectrum typically does not show much difference when compared with an uncollapsed chain.

In this work we use solutions of MEH-PPV primarily in *N*,*N*-dimethylacetamide. We have chosen to work in DMA because it is one of few solvents that will effectively disperse both MEH-PPV and SWCNTs. It is not an aromatic solvent and so will not inhibit phenyl ring rotation along the polymer backbone as described by Traiphol et al.[16] We describe how DMA is not a solvent of high quality for MEH-PPV. We will address the question of MEH-PPV−SWCNT packing/wrapping given flexible SWCNTs and intrinsically stiff straight-chain phenylene-vinylene polymers. In summary, we attempt to enhance the understanding of chemical interactions experienced by SWCNTs and add to the body of evidence associated with energy transfer described by those from Robin Nicholas' group.

Experimental Methods

Materials. The polyphenylenevinylene derivative poly[2-methoxy-5-(2-ethylhexyloxy)-1,4-phenylenevinylene] (MEH-PPV, CAS 138184−36−8, average M_n 40 000−70 000 and polydispersity 6) was purchased from Sigma-Aldrich. *N*,*N*-Dimethylethanamide (DMA) (HPLC grade) solvent was purchased from Sigma-Aldrich. ACS reagent grade chloroform was used as received from J.T. Baker. The chloroform comes with 1% ethanol as a stabilizer. Dry S−P95−03-grade CoMoCat single-wall carbon nanotubes were purchased from Southwest Nanotechnologies Inc., with a quality factor of 0.94 and average tube length of 1 μm. All chemicals were used without further purification. Nanotubes were used as received.

Nanotube−Polymer Solution Preparation. Stock solutions of MEH-PPV were made by adding solvent to dry solid and by subsequent agitation with a Thermolyne type 16700 mixer. Stable stock solutions of SWCNTs were made up using a similar approach to Landi et al.[21] using an ultrasonic bath (VWR, model 75D ultrasonic cleaner, 38.5−40.5 kHz) for 30 min of sonication time at its maximum power setting (90 W average power, 180 W peak power). A 5-min period of sonication of SWCNT stock solutions was used to ensure dispersion homogeneity before MEH-PPV and SWCNT solutions were combined. Mixing was optimized in composite solutions by adding the required volume of stock SWCNT solution to a sample vial containing an appropriate MEH-PPV solution under ultrasonication for these purposes. As soon as solutions were added/mixed the vial was removed from the ultrasonic bath. MEH-PPV was not sonicated for long periods of time to reduce risks of affecting the sample although experiments in our laboratory show that extensive bath sonication of MEH-PPV in DMA has a minimal effect on the photophysics of the MEH-PPV sample.

Solutions for SWCNT fluorescence measurements were made up using horn sonication (Branson digital sonifier model S450, 400 W maximum output used for 15 min with 30% power setting). The sonifier would enhance the debundling of nanotubes such that single tube fluorescence could be observed. Extensive bundling of tubes would result in quenching of SWCNT fluorescence through the likely presence of metallic SWCNTs. Solutions were prepared with a ratio 5 mg SWCNT/6 mg polymer/10 mL solvent (5×10^2 μg/mL SWCNT) in accordance with the experimental procedures described by Hwang et al.[14]

Spectroscopic Methods. UV−vis absorption spectra were recorded with a Shimadzu high resolution UV2401 UV−vis spectrophotometer and with a Perkin-Elmer Lambda 900 UV−vis−NIR spectrophotometer (SWCNT characterization). Fluorescence spectra were collected with a Perkin-Elmer LS-55 using a front surface accessory that compensates for inner filter effects[22] in more concentrated solutions by imaging the volume of solution at the front surface of the cuvette. The fluorescence of SWCNTs was measured using a JY Horiba Fluorolog FL1039 with NIR detection in a front face geometry. All spectra were recorded using 1 cm quartz cuvettes from Starna Cells.

Spectroscopic Fitting. Absorbances of MEH-PPV/SWCNT composite solutions were reconstructed over the full range (300−800 nm) with a combination of, respectively, pure MEH-PPV in DMA and pure as-received CoMoCat SWCNTs in DMA of targeted concentration. In other words, the measured absorbance of a composite dispersion of 0.142 OD MEH-PPV and 7 μg/mL of SWCNT was reconstructed from spectra of 0.142 OD MEH-PPV in DMA and of pure, as-received CoMoCat SWCNT, of concentration 7 μg/mL. The reconstruction was best fit to the measured data over the full spectral range.

The measured spectra were hence corrected for SWCNT absorbance by subtracting the SWCNT absorbance contribution [the coefficients of best fit for the constructed spectra (0.98 ± 0.03 at 95% confidence) for SWCNT absorbance multiplied by actual SWCNT absorbance of the reference dispersion]. This would leave a representation of the MEH-PPV absorbance in that composite dispersion. We also present the difference between raw absorbance data and constructed spectra.

Results and Discussion

Characterization. The fluorescence and absorption spectra of MEH-PPV in solution are shown in Figure 1. It is important to qualify the quality of the solvent, DMA, and the distribution of species that exists in this solvent. For this reason, we demonstrate the absorbance spectra from solutions of MEH-

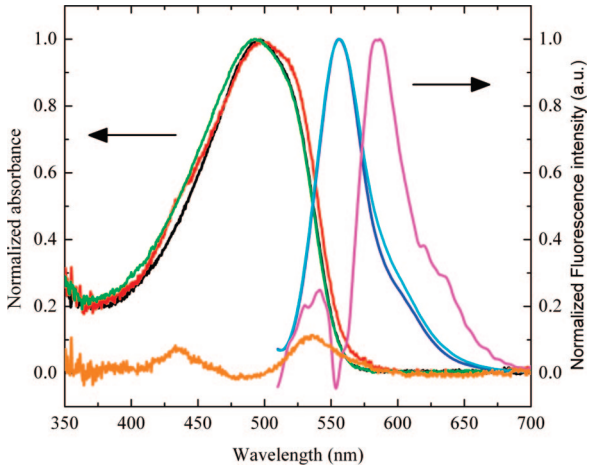

Figure 1. Normalized absorption and fluorescence data of MEH-PPV in 100% chloroform (absorbance of 0.11 at 497 nm, in black, emission in blue), 10% chloroform/90% DMA (absorbance of 0.053 at 497 nm, in red, emission in cyan), and 100% DMA, (absorbance of 0.097 at 492.5 nm, in green). Differences between normalized spectra (10% chloroform/90% DMA absorbance minus 100% chloroform) are shown [absorbance in orange and fluorescence emission (renormalized) in magenta]. All emission spectra were excited at 500 nm and were measured with right angle geometry.

PPV in 100% chloroform by volume, 10% chloroform and 90% DMA by volume, and 100% DMA. We also show in Figure 1 the emission spectra associated with 100% chloroform and 10% chloroform/90% DMA solutions. We highlight differences between the absorbance and emission spectra. All but the absorbance difference spectrum of these curves are normalized to a maximum of one, so that a qualitative assessment can be made.

Upon adding DMA to chloroform, we see the growth of a shoulder on the red edge of the absorbance spectrum along with the growth of a shoulder at 590 nm in the emission. This is direct evidence for the formation of aggregates. The difference spectrum for absorbance peaks at 530 nm and corresponds with the emission "difference" spectrum that peaks at about 590 nm.

We clarify here by stating that MEH-PPV is found as isolated chains in chloroform,[15] a very good solvent for the polymer. When DMA (a relatively poor solvent) is added to the chloroform solution, more aggregation takes place because the polymer chains are initially found in an extended form but are now compelled to minimize interactions with the solvent. When polymer chains are dissolved directly into DMA the fully extended conformation is not likely to ever form as an intermediate. Polymer chains are more likely dissolved in a partially collapsed or agglomerated form.

Consistent with this understanding, we note that the absorbance spectrum of MEH-PPV in 100% DMA has very little evidence of aggregates but shows a much broader blue spectrum indicative of collapsed chains and, to some extent, agglomerates, which tend to have the same optical signature of isolated chains because they are limited in their interchain interaction.[15]

Therefore, in summary we expect a blend of conformational states of MEH-PPV in DMA, but we expect a minor contribution from well-packed-registered (WPR) aggregates. The absorption spectrum of a 5 μg/mL CoMoCat SWCNT dispersion in DMA is shown in Figure 2.

Characterization of the Polymer−NT Composite: Spectral Shift. A series of fluorescence spectra of fixed concentration MEH-PPV and increasing SWCNT concentrations is shown in Figure 3 with selected spectra normalized in Figure 4.

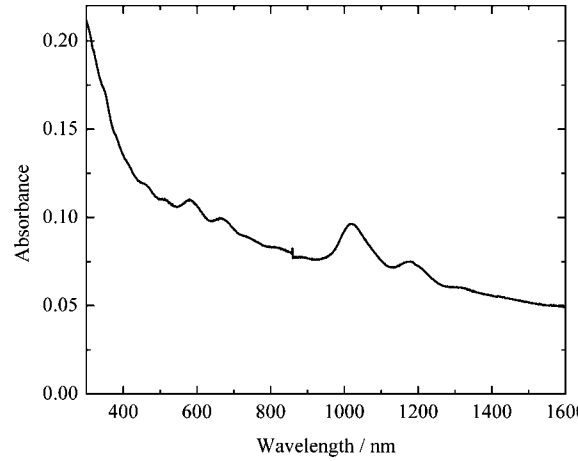

Figure 2. Absorbance of as-received CoMoCat single-walled nanotubes in DMA with a 5 μg/mL target concentration.

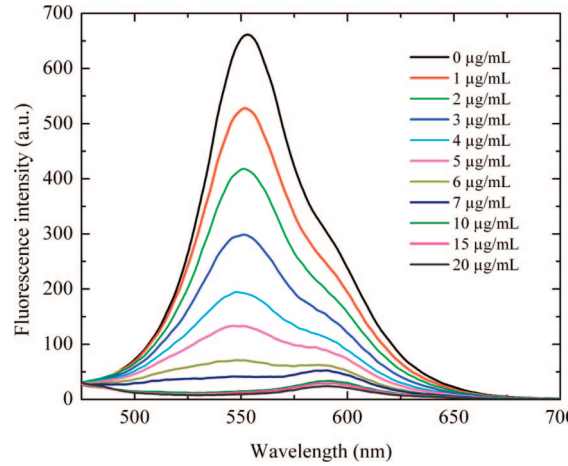

Figure 3. Fluorescence spectra of 0.231 OD MEH-PPV as a function of added CoMoCat SWCNT concentration. The solvent is DMA, and the excitation wavelength is 450 nm.

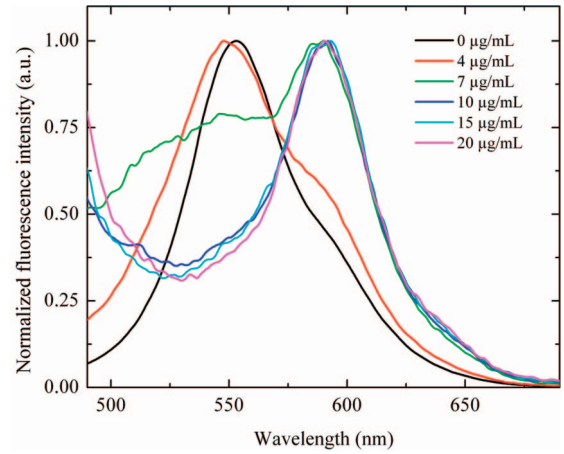

Figure 4. Normalized fluorescence spectra of 0.231 OD MEH-PPV as a function of added CoMoCat SWCNT concentration. The solvent is DMA, and the excitation wavelength is 450 nm.

In Figure 3, we observe a substantial decrease in fluorescence intensity of the MEH-PPV as we add nanotubes to the solution. We also see a red shift as SWCNT concentration increases. It appears that the MEH-PPV is heavily quenched by the SWCNTs. Of note, in previous work, Collison et al.[11] also showed both a decrease in fluorescence intensity and a substantial red shift to 590 nm due to the formation of

aggregates. This aggregate concentration was increasing even as the overall concentration of MEH-PPV remained constant and was caused by a reduction in solvent quality.

The red shift for these same spectra, now normalized, is shown more clearly in Figure 4. This particular presentation only highlights the spectral change and not the decrease in intensity.

On the basis of the data in Figures 3 and 4, we might make the interpretation that either (i) the collapsed chains, isolated chains, and agglomerates are selectively quenched by the nanotubes, or (ii) the distribution of states is changing substantially such that MEH-PPV aggregates completely dominate.

The change in absorbance of the MEH-PPV solution as a function of SWCNT concentration was subsequently measured to gain further insight into the mechanism for fluorescence quenching and red shift. Absorption measurements were made for MEH-PPV/SWCNT in DMA and data are shown in Figure 5a−c.

The raw absorbance data is shown in Figure 5a. The overall absorbance of the dispersions increased over the entire spectral range because of the increase in SWCNT concentration. Absorbance spectra of SWCNT dispersions made up without the presence of MEH-PPV are also provided so that data is more easily and justifiably corrected for SWCNT absorbance. There is some fundamental error associated with the exact concentration of SWCNTs as a result of the less homogeneous nature of SWCNT dispersions. Therefore, the data shown in Figure 5b result from the subtraction of an adjusted SWCNT absorbance spectrum as described in the Experimental Methods section. This allows us to more clearly visualize the true change observed to the MEH-PPV as a result of interaction with the SWCNTs.

When these solutions are made up, the color change is seen clearly by the naked eye. Through UV−vis absorbance measurement the spectrum is seen to red shift with the addition of a shoulder at 570−580 nm. The intensity of this shoulder increases with increasing SWCNT concentration. The spectral peak shifts from 495 nm when there are no SWCNTs present to 520.5 ± 1 nm in the case of 7, 10, and 15 μg/mL solutions. A subtraction of the best fit reconstructed spectra from the measured absorbance of the composite dispersions is shown in Figure 5c, and is quite insightful regarding the spectral changes taking place. There appears to be a small amount of baseline mismatch with these spectra, and so we choose to use this data qualitatively. It is interesting to note the significant decrease in absorbance for these composite solutions below 500 nm along with the growth of the red edge shoulder.

The absorbance red shift corresponds with (i) the substantial red shift seen for the fluorescence (Figures 3 and 4) upon addition of SWCNTs and (ii) low emission efficiency.

Recall that without the addition of SWCNTs, MEH-PPV solutions in DMA alone do not show such a large absorbance due to aggregates, nor is their emission dominated by features at 590 nm. In DMA, there is little evidence for spontaneous formation of WPR aggregates in solutions of MEH-PPV alone. Yet, in this case we could assign red shifts and intensity changes as spectroscopic evidence for the formation of aggregates as SWCNT concentration increases.

In summary, our fluorescence data suggests that, at low SWCNT concentrations, we have fluorescence from all available conformers (and fluorescence from collapsed chains, isolated chains, or agglomerates tends to dominate fluorescence over low-quantum efficiency aggregate fluorescence[11]). As SWCNT concentration increases it appears as if we see a quenching of isolated chains, collapsed chains, and agglomerates or a relative

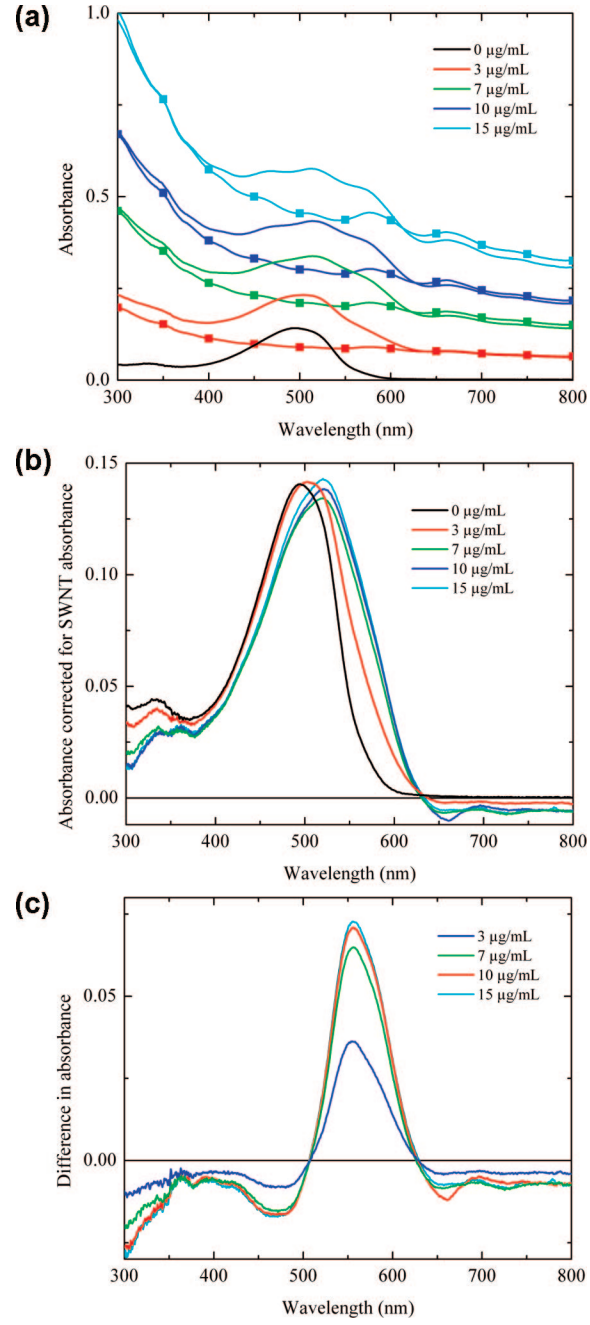

Figure 5. (a) Raw absorbance data of 0.142 OD MEH-PPV in DMA as a function of SWCNT concentration. Lines with squares are the measured absorbance spectra of nanotubes dispersions in DMA, of the appropriate concentration so as to directly compare with composite dispersions spectra. (b) Absorbance of MEH-PPV corrected for SWCNT absorbance for dispersions of varying SWCNT concentration. (c) For dispersions of varying SWCNT concentration we present the difference between raw absorbance data and constructed spectra.

increase in concentration of aggregates WPR chains. Our absorbance data suggests that a relative increase in the concentration of WPR aggregates is occurring at the expense of isolated chains, collapsed chains, and agglomerates. Absorbance is of course sensitive to all conformers, being a good indicator of actual and relative concentrations, but fluorescence is sensitive to the fluorescence quantum efficiency of those conformers. Our absorbance data does not disprove selective quenching of isolated chains, collapsed chains, and agglomerates as a viable interpretation of the fluorescence data of Figures 3 and 4, but it does suggest a substantial increase in the equilibrium constant

associated with WPR aggregate formation, which is puzzling. There is no clear indicator as to the driving force for this change in equilibrium when adding quite small amounts of SWCNTs.

It makes sense to expand our discussion. We expect the MEH-PPV to behave as an isolated chain [a 1-dimensional (1-D) wire] in the best solvent, but when solvent quality is reduced or concentration increases,[11,15,16] generalized 2-dimensional (2-D) and 3-dimensional (3-D) polymer chain overlap takes place. We can consider three mechanisms for 2-D and 3-D polymer overlap: agglomeration, WPR-aggregation, and chain collapse. Increases in concentration of these conformers would occur at constant rates for a given reduction in solvent quality.

With this in mind, Traiphol[15] suggests that a small fraction of all agglomerated chains are WPR chains and that they are randomly distributed. Hence, an increase in WPR aggregates will occur as part of an overall increase in 2-D and 3-D polymer overlap. In other words, we expect an increase in WPR aggregates to occur in addition to increases in collapsed chain or agglomerate concentration. Yet, we find no evidence in our absorbance data for the increase in collapsed chain or agglomerate concentrations. We do instead see a decrease in absorbance below 506 nm and an increase in the absorbance on the red edge, peaking at 556 ± 2 nm (Figure 5c). Our data therefore suggests our chains are aggregating but without an associated chain collapse or agglomeration.

Upon further review, we cannot think of a reason why 2-D and 3-D polymer overlap would increase at all simply by adding SWCNTs. There is no reason to expect formation of collapsed chains, agglomerates, and aggregates unless the MEH-PPV concentration is changing or the solvent quality is reduced, neither of which is taking place.

We conclude that the spectroscopic data observed is not associated with macroscopic solvent phenomena, responsible for distribution changes when adding poor solvents to good solvent solutions of this polymer. There is no evidence to support increased 2-D and 3-D polymer overlap by adding SWCNTs. We therefore need to refine our possible interpretations.

The simplest and most self-consistent explanation for the data is the complexation of polymer and nanotube. Our fluorescence data may be consistent with a selective quenching of collapsed chains, agglomerates, and isolated chains, but we cannot explain the changes in absorbance if this quenching is dynamic quenching, alone. Hence, we propose that the polymer, in all its forms, is complexing with the nanotube. We believe that we are forming SWCNT/MEH-PPV complexes where MEH-PPV chains become restricted in their backbone torsional motion in the same way that occurs with WPR aggregates.[11] The explanation given below is self-consistent with (i) the appearance that we are forming aggregates but not agglomerates and (ii) there being no increase at all in 2-D and 3-D polymer overlap driven by simple addition of SWCNTs.

The explanation is that we have binding along the backbone of the SWCNT. The mechanism that leads to the red shift in MEH-PPV WPR aggregates is the same mechanism that is leading to a red shift in the fluorescence spectrum as a result of complexation between nanotube and polymer. The change observed is consistent with an increase in average conjugation length as MEH-PPV binds to the SWCNT. We interpret the red shift in absorbance in terms of the formation of a ground-state complex between the SWCNT and the conjugated polymer. In this interaction, we suggest that the torsional rotations along the backbone of the polymer chain are restricted because of this interaction with the nanotube.

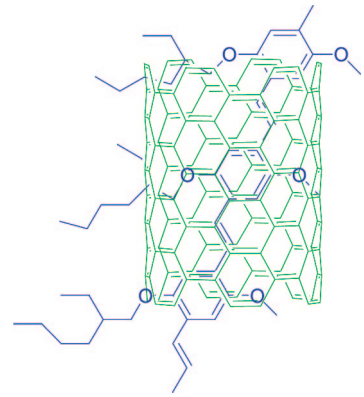

Figure 6. Projectional 2-dimensional sketch of the proposed binding of an MEH-PPV trimer to the backbone of a 6,6 armchair SWCNT to provide a sense of size and scale of the materials involved. The MEH-PPV used is projected to have extended chain lengths of 87−154 nm associated with 130−230 repeat units, and the average nanotube length is projected to be 1000 nm. The orientation of the polymer with respect to the nanotube has been arbitrarily chosen.

Our interpretation, consistent with all the data provided, is summarized below: (1) In DMA a mixture of isolated chains, collapsed chains, agglomerates, and aggregated well-packed registered polymer chains exist. (2) Upon the addition of SWCNTs to the polymer in DMA, the polymer will tend toward forming complexes along the axis of a given SWCNT. All components of the mixture (isolated chains, collapsed chains, agglomerates, and aggregates alike) may indiscriminately interact with the SWCNT with the same result, an average increase in the conjugation length caused by an overall decrease in the torsional rotation along the backbone of the polymer. The driving force for this interaction may include the polymer's energetic requirement to minimize its own interaction with the solvent. For this reason, we suppose the extent of this interaction between polymer and SWCNT will be dependent upon the quality of the solvent. Figure 6 shows, in two dimensions, a sketch of how a polymer chain might interact with a nanotube of chirality 6,6. The sketch allows for a sense of size and scale on an atomic level. The MEH-PPV used is projected to have extended chain lengths of 87−154 nm associated with 130−230 repeat units, and the average nanotube length is projected to be 1000 nm. The orientation of the polymer with respect to the nanotube has been arbitrarily chosen. (3) We hypothesize that energy transfer exists from the higher energy shorter conjugation sequences to the SWCNT but not from the lower energy longer conjugation sequences. With this data alone (Figures 1−5), we cannot conclusively claim that energy transfer originates solely from higher energy sequences. Fluorescence studies (below) of the SWCNT will allow for further consideration of this point. We speculate that interchain interactions (exciplex between polymer and SWCNT) may also occur with long excited-state lifetimes, and the associated high stability that would accompany these lifetimes and time-correlated single photon counting fluorescence measurements will allow us to further test this theory.

In further investigation of the selectivity of energy transfer only from higher energy, shorter conjugation length sequences, we measured fluorescence emission spectra from more concentrated CoMoCat SWCNT/MEH-PPV composite solutions, as a function of excitation wavelength, in an approach similar to that reported by Hwang[14] and Nish.[12] We measured SWCNT fluorescence from dispersions in, first, toluene so that a comparison could be made with this previous work and, second, in DMA. The mixtures of MEH-PPV and SWCNTs were

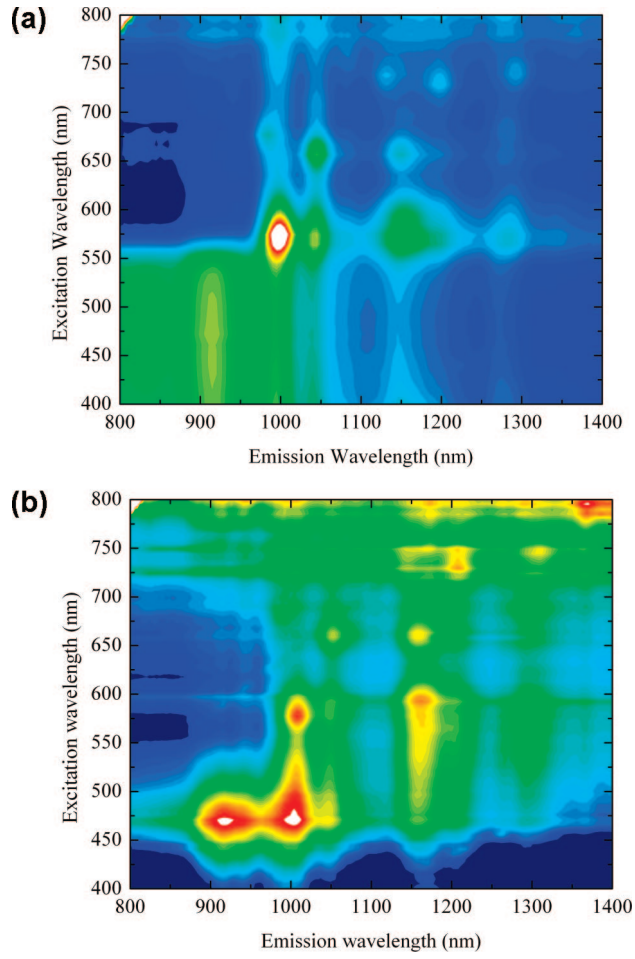

Figure 7. (a) 2-D false color contour plot of SWCNT fluorescence intensity of MEH-PPV/SWCNT composite dispersion in toluene. Fluorescence intensity (counts) is provided as a function of emission and excitation wavelength. Scale runs from 0.0004 counts (navy blue) to 0.0100 counts (white) with lowest measured intensity of 0.0002 counts and highest peak at 0.0135 counts. (b) 2-D false color contour plot of SWCNT fluorescence intensity of MEH-PPV/SWCNT composite dispersion in DMA. Fluorescence intensity (counts) is provided as a function of emission and excitation wavelength. Scale runs from −0.001 counts (navy blue) to 0.0032 counts (white) with lowest measured intensity of −0.00266 counts and highest peak at 0.00342 counts.

dispersed using more aggressive horn ultrasonication approaches. On the basis of previous work,[11,16] we believe the mixture of MEH-PPV in toluene to lean heavily toward isolated chains with longer conjugation lengths compared to a broader mix in the poorer solvent, DMA. Nish also suggested use of toluene in their experiments because of the solvent's ability to dissolve the polymer, which, in turn, would "dissolve" the SWCNT. We suggest the driving force for the SWCNT/MEH-PPV interaction that we describe is simply the polymer's energetic requirement to minimize its interactions with the solvent, a driving force that is not so strong with toluene. However, we are not providing data to confirm this theory in this work.

The data of Figure 7a allows for assignment of fluorescence peaks to the (*n,m*) index of each distinct tube. Standard photoluminescence excitation maps and full assignments can be found,[23,24,12] but for our purposes we concentrate on the (6,5) peak found at ∼575 nm excitation and 1000 nm emission.

Some energy transfer from polymer to SWCNT is suggested by the broad green emission at 1000 nm emission, excited by

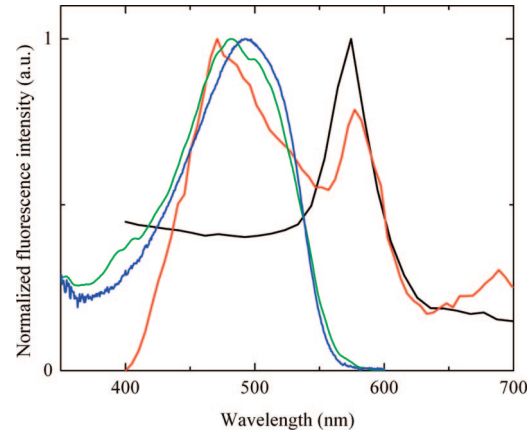

Figure 8. Normalized fluorescence excitation spectra of (i) concentrated MEH-PPV/SWCNT in toluene at 1000 nm emission (black), (ii) concentrated MEH-PPV/SWCNT in DMA at 1001 nm emission (red), (iii) 0.1 OD (dilute) MEH-PPV in DMA at 650 nm emission (green), and (iv) normalized absorbance spectrum of MEH-PPV in DMA (0.097 OD) (blue).

wavelengths 400−550 nm, which overlap with the MEH-PPV absorbance in toluene solution.[11] Any vertical slice of this plot would indicate what spectrum of light was absorbed that would lead to the fluorescence of the tubes assigned. A vertical slice at 1001 nm emission is shown in Figure 8. It can be clearly observed that the bulk of the fluorescence intensity associated with (6,5) tube is as a result of direct excitation of the nanotube. The direct excitation fluorescence peak for this tube at 570 nm is substantially more intense than the fluorescence associated with polymer absorption and subsequent energy transfer (<550 nm excitation).

On the other hand, the data shown in Figure 7b demonstrates that a substantial SWCNT fluorescence at ∼1000 nm emission has originated from excitation of the MEH-PPV and subsequent energy transfer. The normalized fluorescence excitation spectrum in Figure 8 (the vertical slice of 1000 nm emission from Figure 7b) shows substantial overlap with the MEH-PPV in DMA fluorescence excitation spectrum, measured with 650 nm emission, and also with the absorption spectrum of MEH-PPV isolated chains and agglomerates in DMA. Furthermore, in this highly concentrated MEH-PPV solution, this excitation slice taken from the 2-D contour plot has little to no contribution from (those species with optical signature on the red edge of the absorption spectrum) WPR aggregates.

In summary, we interpret this data to suggest the excited states associated with long conjugation length MEH-PPV are not quenched by the nanotubes through energy transfer (irrespective of whether these polymer chains are in direct contact with a nanotube). Solvent quality may also affect the extent of complexation between MEH-PPV and SWCNT, but further investigation is required.

Conclusion

We have shown the value of identifying the different species in solutions of MEH-PPV through recognition of their optical signatures. We have demonstrated that, given the appropriate conditions, CoMoCat SWCNTs and MEH-PPV chains will effectively interact electronically. It will be valuable to assess, in follow-up work, how any driving force to reduce solvent interactions of the polymer will aid in controlling the formation of polymer−nanotube complexes in spin- or drop-cast films. We have shown that the extent of energy transfer from an

excited state (MEH-PPV) to a SWCNT is a function of the type of excited-state species and perhaps the conjugation length. In making measurements of enhanced SWCNT fluorescence in DMA versus in toluene, we have determined that quenching of the excited-state occurs via energy transfer; electron transfer as described by a stepwise Dexter mechanism[25] is not likely given our results. The findings are pertinent to an understanding of the fundamental limitations to electron transfer in polymer photovoltaics that rely on charge separation at the polymer/nanotube interface.

Acknowledgment. We gratefully acknowledge the donors of the American Chemical Society Petroleum Research Fund for partial support of this research. We also thank Rochester Institute of Technology (RIT) for funding of this work through the Department of Chemistry Daniel Pasto Award and through the College of Science Summer Research program. We also thank RIT's Nanopower Resesarch Laboratory (in particular Dr. Ryne Raffaelle and Dr. Brian Landi) for use of instrumentation. We would also like to thank Michael Schettini and Matthew Brister for past contributions to our ongoing work with polymer/SWCNT interactions.

References and Notes

(1) Janssen, R. A. J.; Hummelen, J. C.; Sariciftci, N. S. *MRS Bull.* **2005**, *30*, 33, and references therein.

(2) Terrones, M. *Ann. Rev. Mater. Res.* **2003**, *33*, 419.

(3) Nakayama, K.; Asakura, Y.; Yokoyama, M. *Mol. Cryst. Liq. Cryst.* **2004**, *424*, 217.

(4) Curran, S. A.; Ajayan, P. M.; Blau, W. J.; Carroll, D. L.; Coleman, J. N.; Dalton, A. B.; Davey, A. P.; Drury, A.; McCarthy, B.; Maier, S.; Strevens, A. A. *Adv. Mater.* **1998**, *10*, 1091.

(5) Stéphan, C.; Nguyen, T. P.; de la Chapelle, M. L.; Lefrant, S.; Journet, C.; Bernier, P. *Synth. Met.* **2000**, *108*, 139.

(6) Ago, H.; Petritsch, K.; Shaffer, M. S. P.; Windle, A. H.; Friend, R. H. *Adv. Mater.* **1999**, *11*, 1281.

(7) Raffaelle, R. P.; Landi, B. J.; Harris, J. D.; Bailey, S. G.; Hepp, A. F. *Mater. Sci. Eng., B* **2005**, *116*, 233.

(8) Kymakis, E.; Amaratunga, G. A. J. *J. Appl. Phys. Lett.* **2002**, *80*, 112.

(9) Bhattacharyya, S.; Kymakis, E.; Amaratunga, G. A. J. *Chem. Mater.* **2004**, *16*, 4819.

(10) Collison, C. J.; O'Donnell, M. J.; Alexander, J. L. *J. Phys. Chem. C* **2008**, *112*, 15144.

(11) Collison, C. J.; Rothberg, L. J.; Treemaneekarn, V.; Li, Y. *Macromolecules.* **2001**, *34*, 2346.

(12) Nish, A.; Hwang, J.-Y.; Doig, J.; Nicholas, R. J. *Nanotechnology* **2008**, *19*, 095603.

(13) Nikolaev, P.; Bronikowski, M. J.; Bradley, R. K.; Rohmund, F.; Colbert, D. T.; Smith, K. A.; Smalley, R. E. *Chem. Phys. Lett.* **1999**, *313*, 91.

(14) Hwang, J.-Y.; Nish, A.; Doig, J.; Douven, S.; Chen, C.-W.; Chen, L.-C.; Nicholas, R. J. *J. Am. Chem. Soc.* **2008**, *130*, 3543.

(15) Traiphol, R.; Charoenthai, N.; Srikhirin, T.; Kerdcharoen, T.; Osotchan, T.; Maturos, T. *Polymer* **2007**, *48*, 813.

(16) Traiphol, R.; Sanguansat, P.; Srikhirin, T.; Kerdcharoen, T.; Osotchan, T. *Macromolecules* **2006**, *39*, 1165.

(17) Padmanaban, G.; Ramakrishnan, S. *J. Phys. Chem. B* **2004**, *108*, 14933.

(18) Padmanaban, G.; Ramakrishnan, S. *J. Am. Chem. Soc.* **2000**, *122*, 2244.

(19) Hu, D.; Yu, J.; Padmanaban, G.; Ramakrishnan, S.; Barbara, P. F. *Nano Lett.* **2002**, *2*, 1121.

(20) Szymanski, C.; Wu, C.; Hooper, J.; Salazar, M. A.; Perdomo, A.; Dukes, A.; McNeill, J. D. *J. Phys. Chem. B* **2005**, *109*, 8543.

(21) Landi, B. J.; Ruf, H. J.; Worman, J. J.; Raffaelle, R. P. *J. Phys. Chem. B* **2004**, *108*, 17089.

(22) Kubista, M.; Sjöback, R.; Eriksson, S.; Albinsson, B. *Analyst* **1994**, *119*, 417.

(23) O'Connell, M. J.; Bachilo, S. M.; Huffman, C. B.; Moore, V. C.; Strano, M. S.; Haroz, E. H.; Rialon, K. L.; Boul, P. J.; Noon, W. H.; Kittrell, C.; Ma, J.; Hauge, R. H.; Weisman, R. B.; Smalley, R. E. *Science* **2002**, *297*, 593.

(24) Bachilo, S. M.; Strano, M. S.; Kittrell, C.; Hauge, R. H.; Smalley, R. E.; Weisman, R. B. *Science* **2002**, *298*, 2361.

(25) Lakowizc, J. R. *Principles in Fluorescence Spectroscopy*, 2nd ed.; Springer: New York, 1999.

JP811241V